

# D-carbon: *ab initio* study of a novel potentially superhard carbon allotrope

Dong Fan,<sup>1</sup> Shaohua Lu,<sup>1,\*</sup> Andrey A. Golov,<sup>2</sup> Artem A. Kabanov,<sup>2</sup> and Xiaojun Hu<sup>1,†</sup>

<sup>1</sup>College of Materials Science and Engineering, Zhejiang University of Technology, Hangzhou, 310014, China

<sup>2</sup>Samara Center for Theoretical Materials Science (SCTMS), Samara University, 443011 Samara, Russia

(Dated: April 24, 2018)

By means of *ab initio* computations and global minimum structure search method, we have investigated the structural, mechanical, and electronic properties of D-carbon, a crystalline orthorhombic  $sp^3$  carbon allotrope (space group  $Pnma$  [ $D_{2h}^5$ ] with 6 atoms per cell). Total-energy calculations demonstrate that D-carbon is energetically more favorable than previously proposed T<sub>6</sub> structure (with 6 atoms per cell) as well as many others. This new phase is dynamically, mechanically, and thermally stable at zero pressure, and more stable than graphite beyond 63.7 GPa. The calculations reveal that D-carbon possesses high Vickers hardness (86.58 GPa) and bulk modulus (369 GPa), which are comparable to diamond. D-carbon is a semiconductor with a band gap of 4.33 eV, less than diamond's gap (5.47 eV). The simulated X-ray diffraction pattern is in satisfactory agreement with the previous experimental data in chimney or detonation soot, suggesting its possible presence in the specimen. Finally, we proposed a possible reaction route from the polyethylene chain structure to D-carbon, indicating a plausible approach to synthesize this new phase.

## INTRODUCTION

Carbon is an amazing and versatile element: not only because it is significant and essential element required for all life processes, but also, due to its rich physical and chemical properties. The discovery of fullerenes,[1] nanotubes,[2] and graphene[3] has motivated tremendous interest in recent years to explore newly carbon structures in  $sp^3$ -,  $sp^2$ -, and  $sp$ -hybridized bonding networks. These synthesized carbon allotropes give rise to enormous scientific and technological impacts on natural science, leading to many applications in different fields such as protective coatings, gas sensing, energy storage systems, and solar cells.[4, 5] On the other hand, to guide experimental synthesis of new carbon allotropes, highly accurate theoretical predictions are indispensable in the search of new carbon forms. To our knowledge, various elusive carbon allotropic modifications have been proposed, including the Cco C<sub>8</sub>,[6] bco C<sub>16</sub>,[7] bcc C<sub>8</sub>,[8] T-carbon,[9] T<sub>6</sub>-, and T<sub>14</sub>-carbon[10]. Several predicted carbon phases, *e.g.*, monoclinic bct C<sub>4</sub>,[11] and M-carbon[12] were also proposed to simulate the synthesized phase. Samara Carbon Allotrope Database (SACADA)[13, 14] already indexed more than 500 hypothetical carbon structures and this number is growing fast. And it's worth noting that the previously theoretical predicted T-carbon has been synthesized very recently,[15] although this structure is a thermodynamically metastable phase with the high total energy (-7.92 eV per atom).[9] Moreover, there are still other experimental and theoretical efforts made on new carbon materials (*e.g.*, V carbon[16] and compressed glassy carbon[17]). All of the above gives a reason to name the modern time as 'the era of carbon allotropes'.[18]

In this work, on the basis of the first-principles calculations, we present a theoretical investigation of structural, mechanical, and electronic properties of the proposed

new carbon allotrope which we call D-carbon.[19] D-carbon has zeolite net (with jbw topology[20]) and can be described as a mixture of diamond (dia topology) and zeolite (with sra topology[21]) nets as we will discuss later. The calculated results demonstrate that D-carbon, dynamically stable and with a lower energy than some previously reported modifications (*e.g.*, C<sub>20</sub>,[22] T<sub>6</sub>,[10] and T-carbon[9]), has a Vickers hardness 86.58 GPa mildly smaller than diamond (93.7 GPa). A satisfactory match of simulated and measured X-ray diffraction pattern indicates the possible presence of D-carbon in chimney or detonation soot.

## COMPUTATIONAL DETAILS

The search of stable carbon systems, with six atoms per cell, is also performed using the structure particle swarm optimization (PSO) algorithms as implemented in the CALYPSO package.[23–29] The first-principles calculations were based on density functional theory with the generalized gradient approximation (GGA) in the form of Perdew-Burke-Ernzerhof function for exchange-correlation potential.[30] All the calculations were performed using the Vienna *ab initio* Simulation Package (VASP).[31] The energy cutoff of the plane wave was set to 650 eV and the precision of energy convergence was  $10^{-5}$  eV.[32, 33] The atomic positions were fully relaxed until the maximum force on each atom was less than  $10^{-3}$  eV/Å. For a carbon atom,  $2s^2 2p^2$  electrons were considered as the valence electrons. The Brillouin zone was sampled with a  $10 \times 7 \times 6$  Monkhorst-Pack k-points grid for geometry optimization. Phonon dispersions and frequency densities of states (DOS) were performed in the Phonopy package[34] interfaced with the density functional perturbation theory (DFPT)[35] as performed in VASP. For accurate bandgap estimations, we

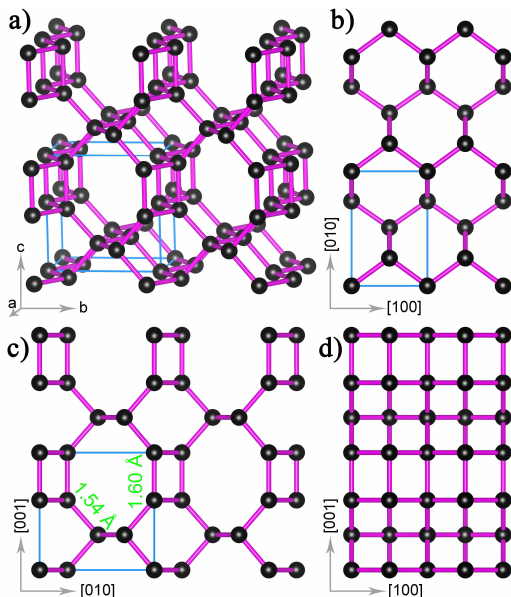


FIG. 1. Crystal structure of D-carbon: a) perspective view, (b-d) view along the  $c$ ,  $a$ , and  $b$  axis, respectively. At zero pressure, lattice parameters of D-carbon are  $a = 2.52 \text{ \AA}$ ,  $b = 3.91 \text{ \AA}$ , and  $c = 3.81 \text{ \AA}$ , occupying the  $2e(0.25 \ 0.00 \ 0.89)$  and  $4k(0.75 \ 0.71 \ 0.38)$  Wyckoff positions, respectively. The unit cell is marked by the blue line, and carbon atoms are plotted with black balls.

employed the hybrid functional approach (HSE06).[36] First-principles finite temperatures molecular dynamics (MD) simulations were performed to further examine the stability of the structure by using time steps of 1 femtosecond in  $3 \times 3 \times 3$  super-cells containing 162 atoms per cell.

## RESULTS AND DISCUSSION

We have performed structure prediction using the PSO methodology for carbon containing six atoms in the simulation cell at 0 K. Besides the well-known graphene,[3]  $T_6$ , [10] and  $T_{12}$ [37] carbon, our simulations also revealed the jbw phase which we call D-carbon. Here, we focus our discussion in this work on only this phase (D-carbon), leaving a detailed analysis of all other predicted metastable structures to a follow-up work.

Fig. 1 displays the optimized structural model of D-carbon. This structure has an orthorhombic primitive cell containing six C atoms, with a highly symmetric space group  $Pmma$  ( $D_{2h}^5$ , 51). At zero pressure, the relaxed bond lengths of C-C are 1.60 and 1.54 Å, respectively. Fig. 2 shows the calculated total energy versus volume and relative enthalpy for D-carbon compared to other previously proposed carbon phases. We note that D-carbon is not only more stable than some theoretically predicted carbon modifications (*e.g.*,  $T_6$ , bcc  $C_8$ ), but

also energetically more favorable than several experimentally realized carbon modifications (*e.g.*,  $C_{20}$  fullerene and T-carbon), implying that the D-carbon could be synthesized. To further evaluate the relative stability of this new phase, we also calculated its cohesive energy  $E_{coh} = [6E_C - E_{total}]/6$ , where  $E_{total}$  and  $E_C$  are the total energy of D-carbon and a single C atom, respectively. As listed in Table S1, the calculated cohesive energy (7.48 eV per atom), apparently higher than recently experimental synthesized T-carbon, (6.573 eV per atom[9, 15]) suggests that D-carbon is a strongly bonding network. We have also compared the relative energy of D-carbon with others known carbon allotropes with 6-atom unit cell (Table S2). As can be seen from Table S2, D-carbon is more stable than many 6-atom structures.

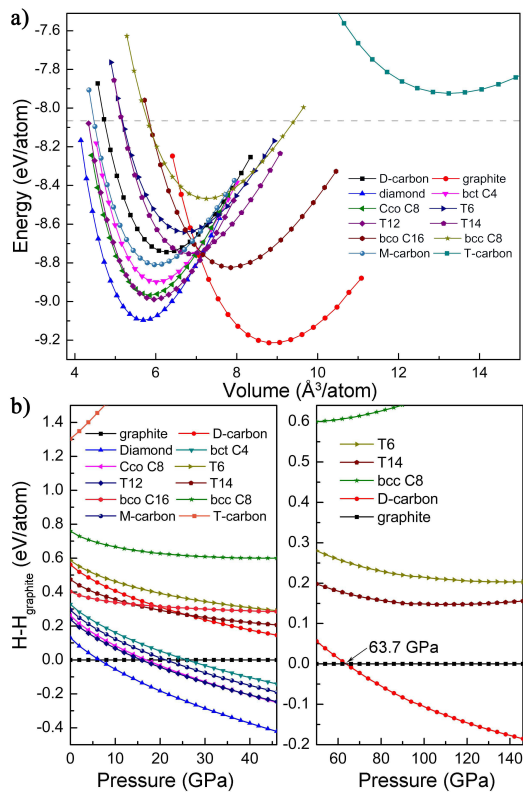


FIG. 2. a) Calculated energy versus volume per atom for D-carbon structure compared to graphite, diamond, bct  $C_4$ , Cco  $C_8$ ,  $T_6$ ,  $T_{14}$ , bco  $C_{16}$ , bcc  $C_8$ , M-carbon, and T-carbon. The dashed line indicates the energy level of  $C_{20}$  fullerene.[22] b) Calculated relative enthalpies of D-carbon, diamond, bct  $C_4$ , Cco  $C_8$ ,  $T_6$ ,  $T_{14}$ , bco  $C_{16}$ , bcc  $C_8$ , M-carbon, and T-carbon with respect to graphite.

Significantly, with the increase of the pressure, the D-carbon becomes preferable to graphite above 63.7 GPa and is more stable than earlier theoretical  $T_6$  and  $T_{14}$  structures at this pressure. (see Fig. 2b) Further, phonon spectrum and phonon density of states (Ph DOS) indicate that D-carbon is dynamically stable, both at zero pressure and high pressure. (see Fig. S1) Therefore,

once synthesized, D-carbon should be quenchable as a metastable phase to ambient pressure and low temperatures. The highest phonon frequency is located at the  $\Gamma$  point with a value of  $\approx 1333 \text{ cm}^{-1}$ , which is lower than graphite ( $\approx 1600 \text{ cm}^{-1}$ ), but close to graphite at 63.7 GPa. The thermal stability of D-carbon was also confirmed by analyzing the backbone root-mean-square deviation (RMSD) from the starting crystal configuration over the process of the trajectory. It is evident that the RMSD levels off to  $\approx 3.7 \text{ \AA}$  at 1000 K, indicating that the geometric configuration is expected to be remarkably stable. (see Fig. S1).

D-carbon has nine independent elastic constants  $C_{ij}$  and for a stable orthorhombic structure its corresponding elastic constants  $C_{ij}$  should satisfy the following elastic stability criteria:  $C_{11}, C_{22}, C_{33}, C_{44}, C_{55}$ , and  $C_{66} > 0$ ,  $[C_{11} + C_{22} + C_{33} + 2(C_{12} + C_{13} + C_{23})] > 0$ ,  $[C_{11} + C_{22} - 2C_{12}] > 0$ ,  $[C_{11} + C_{33} - 2C_{13}] > 0$ , and  $[C_{22} + C_{33} - 2C_{23}] > 0$  for orthorhombic phase.[7] As shown in Table S3, the calculated elastic constants meet this criterion, indicating that it is mechanically stable. The density of D-carbon is  $3.20 \text{ g cm}^{-3}$ , which is comparable to that of bct  $C_4$  ( $3.32 \text{ g cm}^{-3}$ ), but drastically higher than T-carbon ( $1.50 \text{ g cm}^{-3}$ ). (see Table S1) Vickers hardness ( $H\nu$ ) of D-carbon is 86.58 GPa, which is calculated by the empirical formula  $H\nu \text{ (GPa)} = 350[(Ne^{2/3})e^{-1.191fi}]/d^{2.5}$ ,[38] where  $Ne$  is the electron density of the number of valence electrons per cubic angstroms,  $d$  is the bond length, and  $fi$  is the ionicity of the chemical bond in a crystal scaled by Phillips.[39] The calculated Vickers hardness of diamond in this work is 92.49 GPa, closing to the previously theoretical (93.6 GPa) and experimental value ( $96 \pm 5 \text{ GPa}$ ). (see Table S1) According to the generally accepted convention, superhard materials are considered to have a  $H\nu$  exceeding 40 GPa,[40] therefore, D-carbon can be regarded as superhard material.

Stress-strain curves for D-carbon under various strains are shown in Fig. 3a. The ideal strength of D-carbon is strongly anisotropic, and interestingly, tensile stress-strain curves along  $[010]$ ,  $[100]$ , and  $[011]$  show a plastic deformation relation, which is consistent with the ductility of D-carbon compared with diamond. D-carbon with  $[101]$  orientation presents the largest ideal strength of 133 GPa and critical strain reaches to 0.21. However, with  $[011]$  direction, D-carbon shows the smallest ideal strength and critical strain (73 GPa and 0.16), giving rise to the  $(001)$  easy cleavage planes. In the  $(101)$  lattice plane, its pure shear stress along the  $[100]$  direction has the highest peak value (122 GPa), which is moderately lower than  $(111)$ - $[\bar{1}\bar{1}2]$  direction of diamond (140 GPa),[41] but still obviously higher than  $(100)$ - $\langle 001 \rangle$  slip orientation of T-carbon (7.3 GPa),[42] while the  $[0\bar{1}0]$  direction has the lowest peak value (82 GPa). Under indentation shear deformation, the stress response is almost identical to that under pure shear deformation, but pure shear

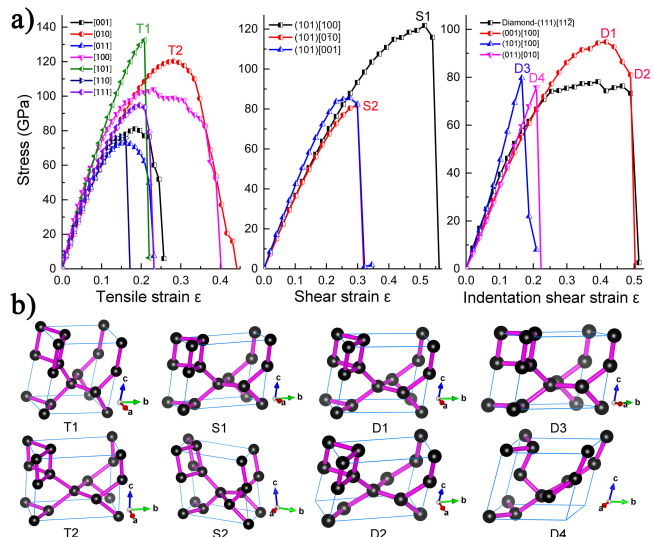


FIG. 3. a) Calculated stress responses under pure tensile, (left) pure shear, (center) and indentation shear (right) strains along various high-symmetry directions, respectively. b) The structural snapshots at different key points after the large deformation of stress on each stress-strain curve under pure tensile, pure shear, or indentation shear strains.

strain causes greatly enhanced stiffness.

Fig. 4a shows the orbitally resolved band structure of D-carbon. It is insulating with an indirect band gap. The PBE band gap is 3.15 eV. The HSE correction does not change the band structure qualitatively, but increases the band gap to 4.33 eV, (see Fig. S2) which is smaller than diamond. The results demonstrate that the valence band maximum (VBM) of D-carbon is contributed by  $C_{2px}$  states, while the conduction band minimum (CBM) is mainly contributed by  $C_{2pz}$  states. There is an obvious orbital hybridization between  $C_{2s}$  and  $C_{2p}$  states below the Fermi level. To investigate the bonding state between the C-C atoms, we calculated its electron localization function (ELF). From Fig. 4b, the D-carbon is an all- $sp^3$  carbon modification with all electrons well localized between the C-C atoms forming the  $\sigma$  bonds.

To further establish the experimental connection of our proposed structure, we have simulated the X-ray diffraction (XRD) patterns to compare with the experimental data. (Fig. 5) Different from diamond where the peaks of  $(111)$  at  $44^\circ$  are observed, for D-carbon, the peaks at  $23.3^\circ$ ,  $32.8^\circ$ , and  $43.1^\circ$  are strong intensity, and one peak at  $22.7^\circ$  with weak intensity is also observed. For chimney or detonation soot, the most distinct feature of the experimental measured XRD spectra is the peak around  $23^\circ$  that does not match any previously known carbon phases.[43, 44] Our simulated XRD results show that the diffraction peak of D-carbon satisfactory match the previously unexplained peak, even though the peaks are broad. These results suggest that D-carbon is a possible candidate of the new carbon phase observed in the chimney

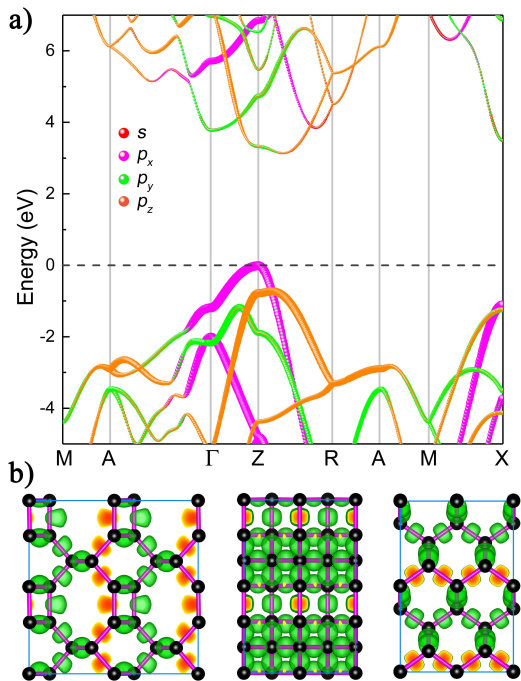


FIG. 4. a) Electronic band structure of D-carbon decomposed with respect to the  $C_s$ ,  $C_{px}$ ,  $C_{py}$ , and  $C_{pz}$  orbitals calculated by PBE functional. b) Calculated ELF of D-carbon at 0 GPa. The isosurface value is set as 0.75.

or detonation soot. The simulated Raman and Infrared (IR) vibrational modes with corresponding frequencies are presented in Fig. S3. The Raman and IR spectra exhibit distinguishing lines at  $1075\text{ cm}^{-1}$  and  $1239\text{ cm}^{-1}$ , respectively. These attainable features may be helpful for identifying the D-carbon experimentally.

To guide the experimental discovery of this novel allotrope, we also proposed a schematic illustration of the possible reaction route for D-carbon structure by using polyethylene chains *via* dehydrogenation and assembly. As shown in Fig. 6, starting from single polyethylene chains,[45, 46] the ultrathin diamond (110)-surface-like frameworks can be formed through dehydrogenation and assembly; Then, with polyethylene chains continued to increase, the distorted  $sp^3$ -hybridized carbon bond can be formed; Finally, the bulk D-carbon framework can be prepared by stacked the polyethylene chains with dehydrogenation and assembly. Therefore, given its energetic more favorable and high dynamic stability, and in consideration of the rapid development in experimental techniques which have synthesized some novel carbon allotropes recently,[15, 16, 47], we expect that D-carbon could be fabricated experimentally in the near future.

Next, we decomposed D-carbon with the jbw topology into building units to find relation between the D-carbon and other three-periodic carbon allotropes from SACADA database. Decomposition was carried out by means of algorithm of searching for the natural tiling[48]

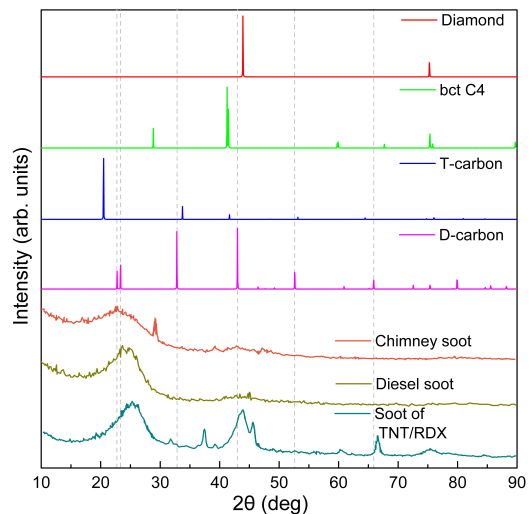


FIG. 5. The simulated XRD patterns of diamond, bct  $C_4$ , T-carbon, and D-carbon, compared with experimental data. The experimental XRD patterns from Ref.[43] and Ref.[44]. The used X-ray wavelength is  $1.54\text{ \AA}$  as employed in the experiment.[44]

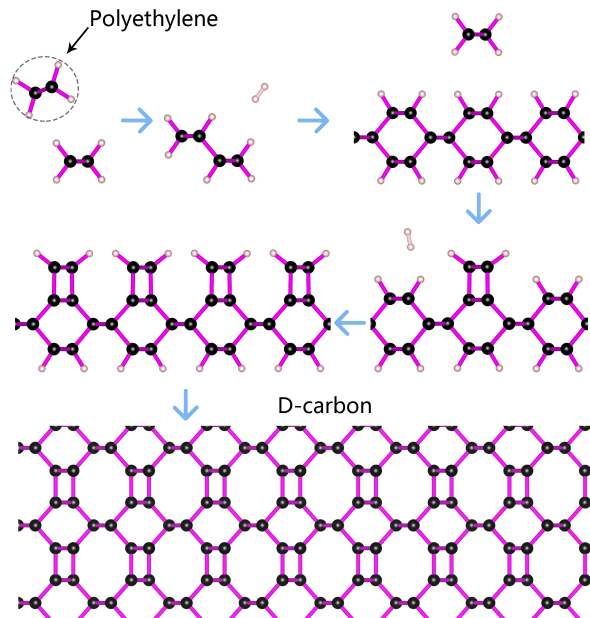


FIG. 6. Schematic illustration of the formation of the D-carbon. Black and white represent carbon and hydrogen atoms, respectively.

that is implemented in the ToposPro[49] program package. The 3dt[50] program was used for visualisation of the building units and way of its assembling. As has been previously shown the tiling approach can be useful to predict as well as classify and compare allotropes.[51]

The jbw net is constructed from two types of building units in a one-to-one ratio, adamantane cage  $4^6$  (which formed by four six-member ring) of diamond (Fig. 7a)

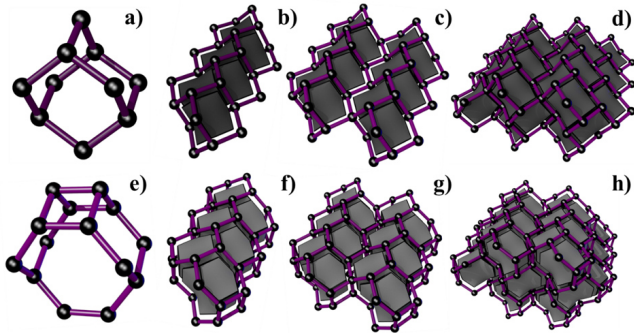


FIG. 7. The building schemes of diamond (a - d) and sra (e - h) nets.

and  $4^2.6^2.8^2$  cage (Fig. 7e) of sra net. The  $4^2.6^2.8^2$  cage can be considered as extended the  $4^6$  adamantane cage. Due to close geometry and topology of the building units diamond and sra nets have the same way of self-assembling (Fig. 7). The building blocks are connecting to each other through common 6- (Fig. 7b) and 8-membered rings (Fig. 7f), respectively and form one-periodic chains. The chains are joined in two-periodic layers by means of common zigzag-like simply connected (Fig. 7c) and ladder (Fig. 7g) chain. Finally, the nets are assembling from the layers through common 6-membered rings (Fig. 7d, h).

In both cases the external surface of the dia and sra layers is distorted graphene-like surface. Consequently, the layers are complementary and can be used to construct new nets. Theoretically infinite number of topologically inequivalent nets can be obtained by means of various combination of the layers. However, only a few of such nets (Fig. 8) were reported as a possible carbon allotropes: jbw, mbc-4,4-Imma and  $4^3T190$ .

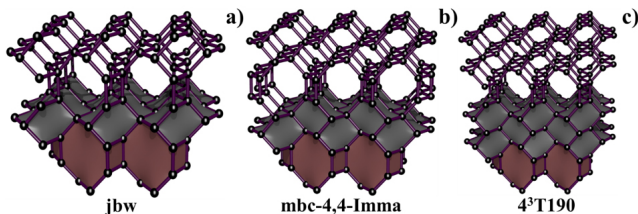


FIG. 8. The assembling schemes of jbw a), mbc-4,4-Imma b), and  $4^3T190$  c) nets from diamond (grey) and sra (brown) layers.

All these allotropes are hybrids of diamond and carbon structures with sra topology, which was firstly reported as 8-tetra(3,3)tubulane. In this way the allotropes should have intermediate properties between diamond and 8-tetra(3,3)tubulane (Table S4). The structure of the diamond has the lowest energy and the higher density in comparison with the structure of the

8-tetra(3,3)tubulane. As a result, the increase of amount of diamond layers in the structures decreases energy and increases the density (Table S4) of the allotropes.

## CONCLUSIONS

In summary, the D-carbon, an orthorhombic  $sp^3$  bonded structure, was studied theoretically using *ab initio* calculations and unbiased structure searching techniques. This structure is energetically more stable than several previously proposed  $sp^3$  carbon allotropes with 6 atoms per cell. The results in this work indicate that D-carbon is another potential modification of metastable  $sp^3$  carbon system. Possible synthesis routes are also proposed. Our work not only determines a previously unrecognized carbon allotrope with rare structural motifs and high dynamic stabilities, but also promote future studies to explore new carbon allotropes with novel electronic and mechanical properties.

## ACKNOWLEDGEMENTS

This work was supported by the National Natural Science Foundation of China (Grant Nos. 11504325, 50972129, and 50602039), and Natural Science Foundation of Zhejiang Province (LQ15A040004). This work was also supported by the international science technology cooperation program of China (2014DFR51160), the National Key Research and Development Program of China (No. 2016YFE0133200), the European Union's Horizon 2020 Research and Innovation Staff Exchange (RISE) Scheme (No. 734578), and the One Belt and One Road International Cooperation Project from Key Research and Development Program of Zhejiang Province (2018C04021). A.A.K. thanks the Russian Foundation for Basic Research for a partial support with grant #16-32-00296 mol\_a and the Russian Ministry of Science and Education for a partial support with grant #3.7626.2017/9.10 The authors gratefully acknowledge the suggestions and advice of Prof. D.M. Proserpio.

\* [lsh@zjut.edu.cn](mailto:lsh@zjut.edu.cn)

† [huxj@zjut.edu.cn](mailto:huxj@zjut.edu.cn)

- [1] W. Krätschmer, L. D. Lamb, K. Fostiropoulos, and D. R. Huffman, *Nature* **347**, 354 (1990).
- [2] S. Iijima and T. Ichihashi, *nature* **363**, 603 (1993).
- [3] K. S. Novoselov, A. K. Geim, S. V. Morozov, D. Jiang, Y. Zhang, S. V. Dubonos, I. V. Grigorieva, and A. A. Firsov, *science* **306**, 666 (2004).
- [4] J. Lee, J. Kim, and T. Hyeon, *Advanced Materials* **18**, 2073 (2006).
- [5] A. A. Balandin, *Nature materials* **10**, 569 (2011).

- [6] Z. Zhao, B. Xu, X.-F. Zhou, L.-M. Wang, B. Wen, J. He, Z. Liu, H.-T. Wang, and Y. Tian, *Physical review letters* **107**, 215502 (2011).
- [7] J.-T. Wang, H. Weng, S. Nie, Z. Fang, Y. Kawazoe, and C. Chen, *Physical review letters* **116**, 195501 (2016).
- [8] R. L. Johnston and R. Hoffmann, *Journal of the American Chemical Society* **111**, 810 (1989).
- [9] X.-L. Sheng, Q.-B. Yan, F. Ye, Q.-R. Zheng, and G. Su, *Physical review letters* **106**, 155703 (2011).
- [10] S. Zhang, Q. Wang, X. Chen, and P. Jena, *Proceedings of the National Academy of Sciences* **110**, 18809 (2013).
- [11] K. Umemoto, R. M. Wentzcovitch, S. Saito, and T. Miyake, *Physical review letters* **104**, 125504 (2010).
- [12] Q. Li, Y. Ma, A. R. Oganov, H. Wang, H. Wang, Y. Xu, T. Cui, H.-K. Mao, and G. Zou, *Physical review letters* **102**, 175506 (2009).
- [13] R. Hoffmann, A. A. Kabanov, A. A. Golov, and D. M. Proserpio, *Angewandte Chemie International Edition* **55**, 10962 (2016).
- [14] (<http://sacada.sctms.ru>).
- [15] J. Zhang, R. Wang, X. Zhu, A. Pan, C. Han, X. Li, D. Zhao, C. Ma, W. Wang, H. Su, *et al.*, *Nature communications* **8**, 683 (2017).
- [16] X. Yang, M. Yao, X. Wu, S. Liu, S. Chen, K. Yang, R. Liu, T. Cui, B. Sundqvist, and B. Liu, *Physical review letters* **118**, 245701 (2017).
- [17] M. Hu, J. He, Z. Zhao, T. A. Strobel, W. Hu, D. Yu, H. Sun, L. Liu, Z. Li, M. Ma, *et al.*, *Science advances* **3**, e1603213 (2017).
- [18] A. Hirsch, *Nature materials* **9**, 868 (2010).
- [19] V. L. Deringer, G. Csányi, and D. M. Proserpio, *ChemPhysChem* **18**, 873 (2017).
- [20] A. Healey, P. Henry, G. Johnson, M. Weller, M. Webster, and A. Genge, *Microporous and mesoporous materials* **37**, 165 (2000).
- [21] V. Blatov, L. Carlucci, G. Ciani, and D. Proserpio, *CryStEngComm* **6**, 377 (2004).
- [22] H. Prinzbach, A. Weiler, P. Landenberger, F. Wahl, J. Wörth, L. T. Scott, M. Gelmont, D. Olevano, and B. v. Issendorff, *Nature* **407**, 60 (2000).
- [23] Y. Wang, J. Lv, L. Zhu, and Y. Ma, *Physical Review B* **82**, 094116 (2010).
- [24] Y. Wang, J. Lv, L. Zhu, and Y. Ma, *Computer Physics Communications* **183**, 2063 (2012).
- [25] L. Zhu, H. Liu, C. J. Pickard, G. Zou, and Y. Ma, *Nature chemistry* **6**, 644 (2014).
- [26] Y. Li, J. Hao, H. Liu, Y. Li, and Y. Ma, *The Journal of chemical physics* **140**, 174712 (2014).
- [27] H. Wang, S. T. John, K. Tanaka, T. Itaka, and Y. Ma, *Proceedings of the National Academy of Sciences* **109**, 6463 (2012).
- [28] J. Lv, Y. Wang, L. Zhu, and Y. Ma, *Physical Review Letters* **106**, 015503 (2011).
- [29] L. Zhu, H. Wang, Y. Wang, J. Lv, Y. Ma, Q. Cui, Y. Ma, and G. Zou, *Physical Review Letters* **106**, 145501 (2011).
- [30] J. P. Perdew, K. Burke, and M. Ernzerhof, *Physical review letters* **77**, 3865 (1996).
- [31] G. Kresse and J. Furthmüller, *Physical review B* **54**, 11169 (1996).
- [32] D. Fan, S. Lu, Y. Guo, and X. Hu, *Journal of Materials Chemistry C* **5**, 3561 (2017).
- [33] D. Fan, S. Lu, Y. Guo, and X. Hu, *Journal of Materials Chemistry C* **6**, 1651 (2018).
- [34] A. Togo and I. Tanaka, *Scripta Materialia* **108**, 1 (2015).
- [35] S. Baroni, S. De Gironcoli, A. Dal Corso, and P. Gianozzi, *Reviews of Modern Physics* **73**, 515 (2001).
- [36] J. Heyd, G. E. Scuseria, and M. Ernzerhof, *The Journal of chemical physics* **118**, 8207 (2003).
- [37] Z. Zhao, F. Tian, X. Dong, Q. Li, Q. Wang, H. Wang, X. Zhong, B. Xu, D. Yu, J. He, *et al.*, *Journal of the American Chemical Society* **134**, 12362 (2012).
- [38] F. Gao, J. He, E. Wu, S. Liu, D. Yu, D. Li, S. Zhang, and Y. Tian, *Physical review letters* **91**, 015502 (2003).
- [39] J. Phillips, *Reviews of Modern Physics* **42**, 317 (1970).
- [40] V. L. Solozhenko, D. Andrault, G. Fiquet, M. Mezouar, and D. C. Rubie, *Applied Physics Letters* **78**, 1385 (2001).
- [41] Y. Zhang, H. Sun, and C. Chen, *Physical Review B* **73**, 144115 (2006).
- [42] X.-Q. Chen, H. Niu, C. Franchini, D. Li, and Y. Li, *Physical Review B* **84**, 121405 (2011).
- [43] P. Chen, F. Huang, and S. Yun, *Carbon* **41**, 2093 (2003).
- [44] D. Pantea, S. Brochu, S. Thiboutot, G. Ampleman, and G. Scholz, *Chemosphere* **65**, 821 (2006).
- [45] B. Montanari and R. Jones, *Chemical physics letters* **272**, 347 (1997).
- [46] A. Henry and G. Chen, *Physical review letters* **101**, 235502 (2008).
- [47] P. Liu, H. Cui, and G. Yang, *Crystal Growth and Design* **8**, 581 (2008).
- [48] V. A. Blatov, O. Delgado-Friedrichs, M. O’Keeffe, and D. M. Proserpio, *Acta Crystallographica Section A: Foundations of Crystallography* **63**, 418 (2007).
- [49] V. A. Blatov, A. P. Shevchenko, and D. M. Proserpio, *Crystal Growth & Design* **14**, 3576 (2014).
- [50] (<http://gavrog.org/>).
- [51] I. A. Baburin, D. M. Proserpio, V. A. Saleev, and A. V. Shipilova, *Physical Chemistry Chemical Physics* **17**, 1332 (2015).